

# Microscope studies of the morphology and structure of carbon nanotubes

SISHEN XIE, NAN LI, ZEBU ZHANG, WEI LIU, GANG WANG,  
SHENGFA QIAN, CHUNSHENG FU

*Institute of Physics, Chinese Academy of Sciences, Beijing, 100080, People's Republic of China*

We have studied the morphologies and structures of carbon nanotubes (bucky-tubes) and carbon nanoparticles (buckyonions) using scanning electron microscopy (SEM), high resolution transmission electron microscopy (HRTEM) and scanning tunnelling microscopy (STM). By SEM the carbon nanotubes are observed with features similar to those of some fibrous whiskers grown from pyrolytic graphite. This growth feature is supported by transmission electron microscopy (TEM) observations. The TEM results show also that the graphitic sheets can be bent into curved shapes to cap the nanotubes or form the onions. In the curved graphitic sheets elastic strains induced by layer mismatches and dislocations are revealed. The STM observations on the nanotubes show a bundle-like morphology of the carbon nanotubes, and by atomic resolution images the zigzag and armchair atomic configurations may be identified. The results also show structural distortions which may be produced by folding the graphite sheets to create the nanotubes and are responsible for the lattice mismatch.

## 1. Introduction

Carbon nanotubes have been the focus of intense interest since their recent discovery [1–3]. This attention has been intensified considerably after Ajayan and Iijima [4] developed a method for producing carbon nanotubes in gram quantities. Practical usefulness of this material as composite, catalysts, and molecular wires has been suggested by many authors, its potential importance in technology as the basis of intrinsically conducting one-dimensional polymers has been predicted by theoretical considerations. By transmission electron microscopy (TEM) and electron diffraction, the structures of carbon nanotubes have been investigated [1–6]. These studies confirm that the carbon nanotubes are composed of concentric cylinders of hollow carbon hexagonal networks arranged around one another, often with helical twists [6, 7]. In addition, the cylindrical tubes are closed, in most cases, with some other polygons such as pentagons or heptagons [5]; some of them are first transformed into a conical shape before being enclosed.

In this work, we present a series of experimental observations on carbon nanotube structures. Scanning electron microscopy (SEM), high-resolution transmission electron microscopy (HRTEM) and scanning tunnelling microscopy (STM) are used in the structural investigations. By these methods, morphologies and some structural details of the carbon nanotubes are shown wherein defects and structural deformations are revealed.

## 2. Experimental procedure

The carbon nanotubes and nanometre sized particles, which have been known as buckyonions, are produced in gram quantities with an arc discharge method similar to that of Ebbesen and Ajayan [8]. Details of the experimental conditions have been described elsewhere [9]. During the arc discharge, graphitic carbon is deposited and accumulates on the surface of the graphite electrodes. Cutting through the deposit, large amounts of nanotubes and onions can be found in the cone region of the soft black deposit.

## 3. Results and discussion

### 3.1. SEM observations

Fig. 1 shows a set of SEM images obtained on the carbon nanotubes. In Fig. 1(a) a cross-section view of a deposit in rod shape is exhibited, in which a shell-like structure can be clearly observed. In the transition region between the shell layers, as indicated by a white square, large amounts of nanotubes and onions are found. Fig. 1(b) is a zoomed picture around the white square in Fig. 1(a), that shows the morphology of carbon nanotubes found there. Usually the nanotubes appear as straight rods with their sizes varying between 5–50 nm in diameter and several micrometres in length, though some bent tubes can also be seen. From Fig. 1(b) it is observed that the nanotubes are attached, in most cases, to the pyrolytic graphite at one end. This morphology suggests a free-end growth mechanism for the nanotubes. In addition, the fact

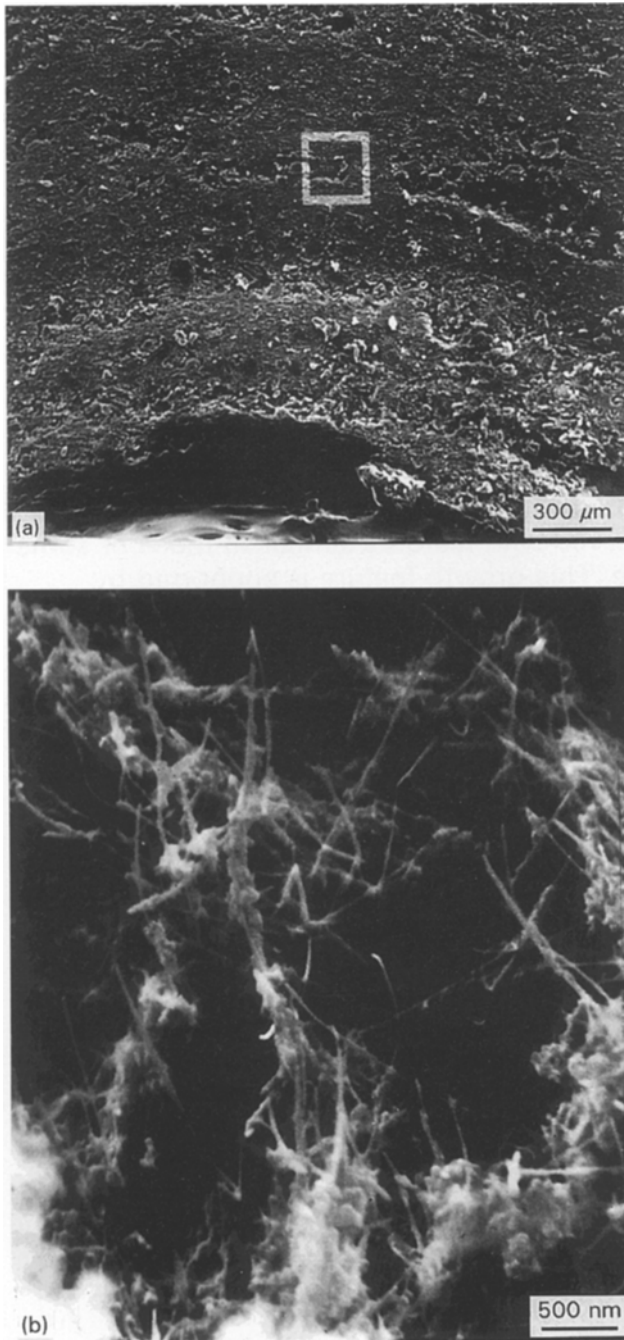


**Figure 1** (a) An SEM image of a cross-section of the typical rod-shaped deposit produced by arc discharge of graphite electrodes. (b) A high magnification SEM image of the carbon nanotubes found in the rod-shaped deposit in the place shown by the white square in (a).

that the carbon nanotubes are found only in the porous region in the deposit shell implies a similar situation to vapour-grown crystals for the carbon nanotubes.

### 3.2. TEM observations

For TEM observations, soft black powders are collected from the core region of the rod-shape deposit. The powders are further ground and treated in an ultrasonic bath of acetone. After that, they are dispersed on a carbon TEM grid with holes. The HRTEM studies are carried out with a Jeol-200 CX system.

By TEM, carbon nanotubes and onions in various shapes, such as tubes with a varying number of shells or with regular cone-like terminations, are frequently observed. Meanwhile, disordered carbon layers (turbostratic graphite) are also seen on the outer surfaces of the nanotubes, as shown in Fig. 2(a). This result is in concurrence with that observed by SEM. The incomplete and terminated graphitic layers on the carbon nanotube seem to suggest a sudden interruption of a simultaneous growth process for both the inside and outside graphitic layers. This can be attributed to a very unstable growing process at the very high temperature of  $\sim 2500^\circ\text{C}$  near the arc. Alternatively, this result can also be understood as that the nanotubes grow from the carbon deposit consisting mainly of pyrolytic graphite with residual amorphous carbon, since the very high temperature near the arc favours graphitization. These residual amorphous carbon and pyrolytic graphite fragments can actually be seen in Fig. 2(a). By a careful observation of Fig. 2(a), we consider that both of the processes for the carbon nanotube growth may exist in the arc discharge procedure.

Fig. 2(b) shows a typical fragment of pyrolytic graphite composed of many graphitic layers. A peculiar structure can be observed in the picture that at the fragment edge the graphitic layers are enclosed with bent sheets which form a curved enclosure. The mechanism for the formation of the curved enclosure is still unknown, but it may be supposed that if the curved enclosures at the fragment edge are broken and isolated from the fragment, they may form onions when they complete the reconstruction and are enclosed at the other end. These forms of polyhedral particles are frequently observed in our TEM observations. One of such images is shown in Fig. 2(c). The observed onions are usually sized between 5–40 nm and consist of five or more curved graphite sheets. For the particular one shown in Fig. 2(c) it is observed that the onion has a hexagonal shape on its projection plane. On its outer surface unclosed graphitic sheets are involved. It has been indicated by Dravid *et al.* [10] that broken nanotubes can be the precursors to onion formation. Thus the unclosed graphitic sheets on the outer surface of the onion can be a hint to indicate a possible growth mechanism.

In Fig. 2(d) the enclosure end of a nanotube is exhibited. Image contrast can be clearly observed in the picture and steps of graphitic sheet are also shown. Furthermore, a particular triangle region, which has a symmetry around the tube axis, is involved in the enclosure end. All these observed features can be attributed to elastic strains due to the curvature of graphitic layers and dislocations and mismatches, occurring around the boundary of the triangle region, among the layers. In Fig. 2(d) it can also be observed that a few curved graphite layers appear on the outer surface of the tube apex which are terminated abruptly. This means that extra graphitic layers are attached to the surface of the tube apex. This type of surface structure is also known with PAN-based carbon fibres.

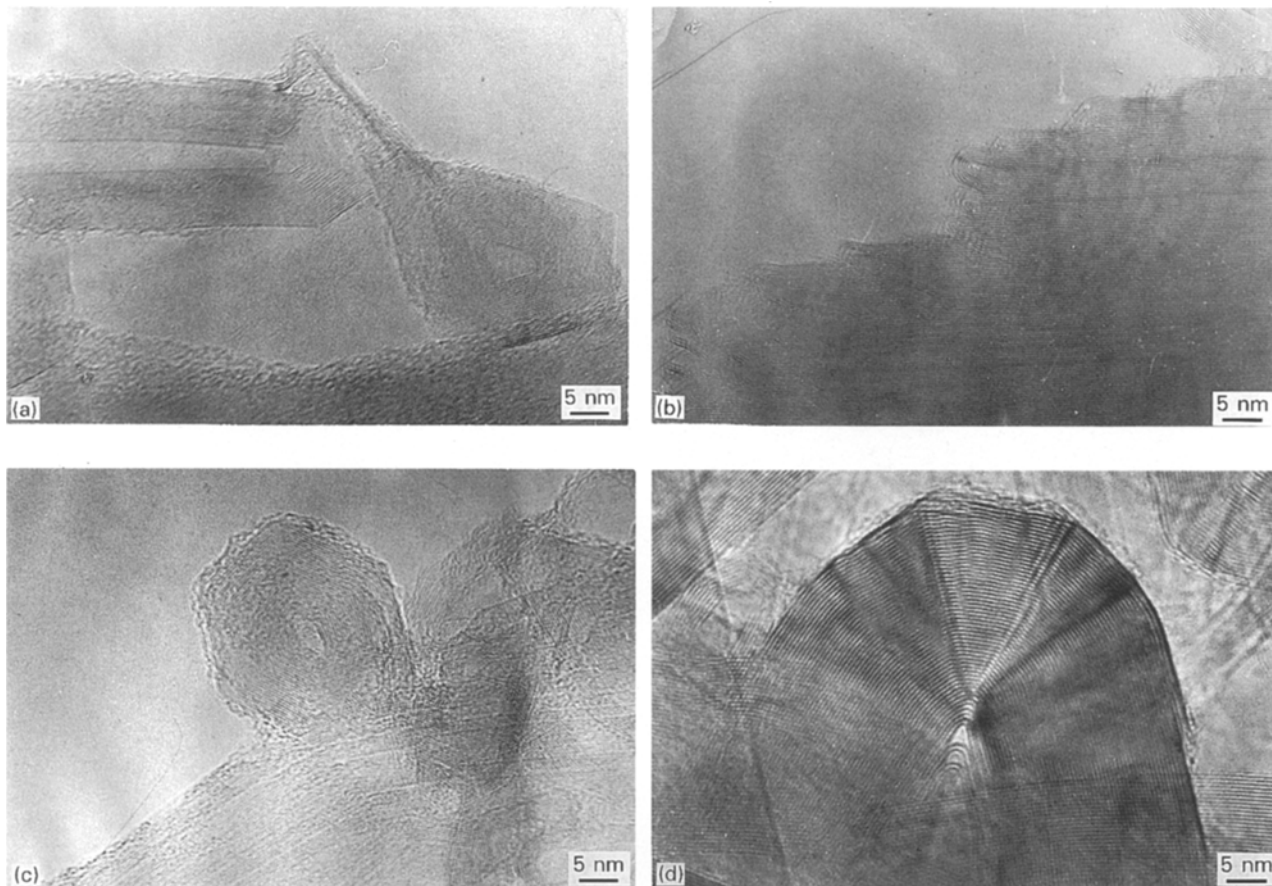


*Figure 2* TEM images of the carbon nanotubes and onions. (a) Two tubes with amorphous carbon at their open ends and on their outer surfaces. (b) A typical fragment of pyrolytic graphite composed of many graphitic layers. The graphitic layers are enclosed with bent sheets which form a curved enclosure at the fragment edge. (c) Onions in a hexagonal shape with many curved graphite sheets. The size of the onion is  $\sim 25$  nm in diameter. (d) A high resolution image of the enclosure end of a nanotube with clear image contrast. Particular triangle regions with symmetry around the tube axis are involved in the enclosure end, and steps of graphitic sheet are clearly shown.

### 3.3. STM observations

For STM measurement the carbon deposit produced in arc discharge is also ground into a powder and treated in an ultrasonic bath of acetone. The powder is further dispersed in methylic benzene to make a suspended solution. Droplets of the solution are placed on newly cleaved graphite surfaces and dried in air. Then, the nanotube samples are available for STM study with our Model DS-89 STM system (made in Beijing University). The STM scanning was generally been carried out in constant current (CC) mode at bias voltages of  $-200$  mV to  $-600$  mV and tunnelling currents of  $0.2$ – $1.0$  nA. Electrochemically etched tungsten tips were used and the scanning was performed in air at room temperature.

Fig. 3(a) shows a  $150 \times 150$  nm overview of the carbon nanotubes obtained on one sample surface with STM. It is seen from the image that the nanotubes usually combine in a bundle and align in nearly the same direction. This can be understood since they are produced in the same current flow direction in the arc discharge. The tubule lengths exceed the scan range, while their diameters vary from  $\sim 4.0$  nm to  $\sim 16$  nm. The morphologies of the tubules are not very smooth. This can be attributed to the existence of broken bits of graphite produced during arc discharge or sample grinding, which may considerably affect the imaging process.

In Fig. 3(b) a  $45 \times 45$  Å atomic resolution image obtained around one tubule in Fig. 3(a) is exhibited. In the image rows of carbon atoms are observed in the lower right region. It is determined, with the help of the protruding landmark, that one direction of the atom rows, from the left of the image to the upper right, is about  $30^\circ$  from the tubule axis. This orientation suggests a zigzag structure, where one C–C bond in hexagons of the nanotubes is parallel to the tubule axis, for the observed nanotubule. It is determined that the atom row spacing is about  $2.1$  Å, which agrees well with the  $2.13$  Å row separation of carbon atoms in the STM image of graphite. This presents evidence for the identification of the zigzag configuration for the nanotubule. In Fig. 3(c) a schematic diagram of the zigzag configuration is given in which the relative direction of the atom rows with respect to the nanotubule axis is shown.

In Fig. 3(d) an STM image of the nanotubes from another sample surface is given. The  $150 \times 150$  nm overview shows that the tubules are also combined in a bundle and aligned in the same direction. Their lengths also exceed the scan range and their diameters vary from  $\sim 2.5$  nm to  $\sim 9.0$  nm. In Fig. 3(e), a  $42 \times 42$  Å image around one tubule in Fig. 3(d) is displayed. Around the middle of the image, rows of carbon atoms are clearly seen, which can be divided into a lower part with a row image similar to that of

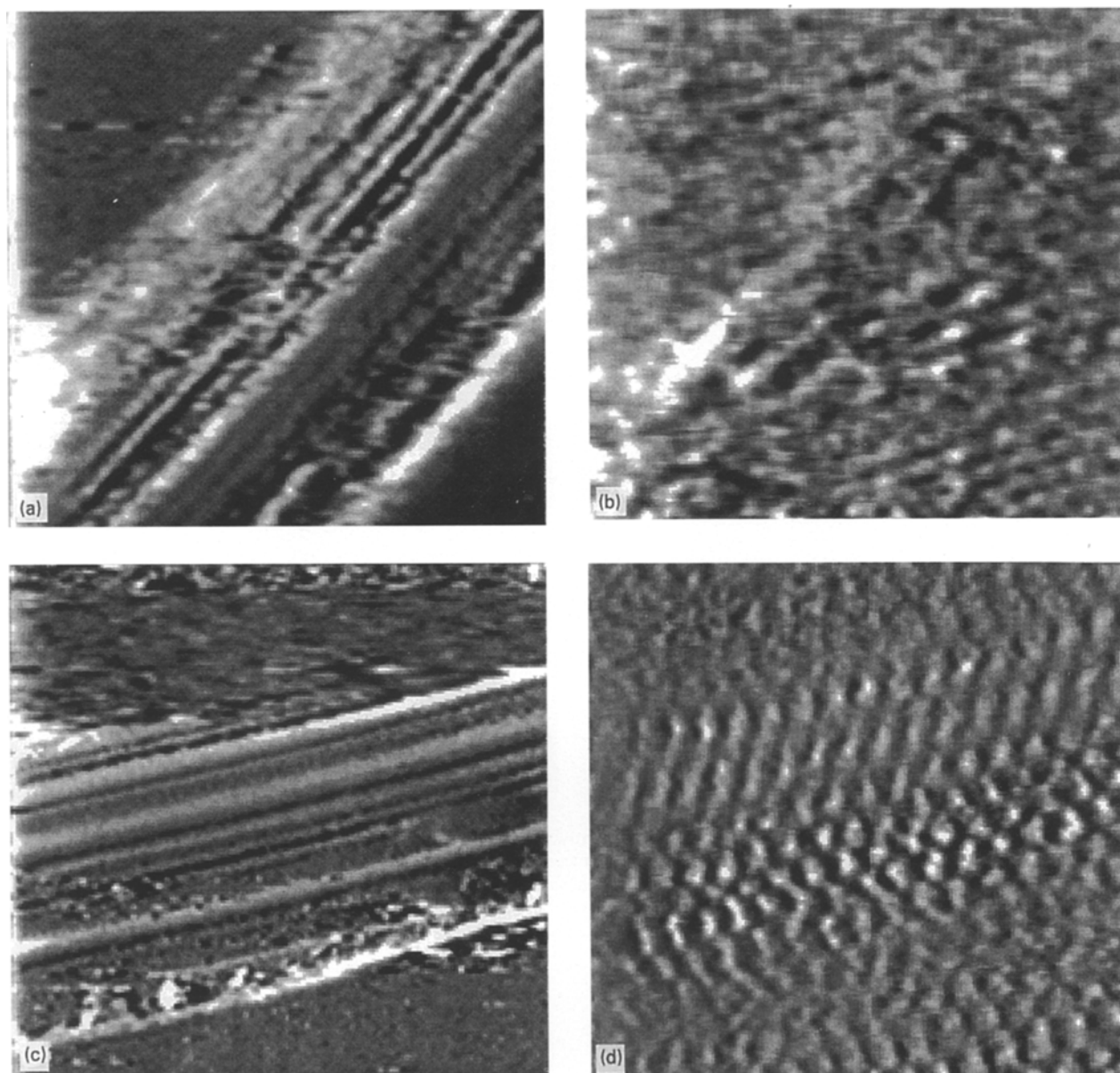


**Figure 3** STM images of carbon nanotubes taken in constant current mode. (a) A  $150 \times 150$  nm overview on one sample surface. The bias voltage is  $V_m = -560$  mV and the tunnelling current  $I_t = 0.21$  nA. (b) An atomic scale image of  $45 \times 45$  Å on one tubule in (a). The image was taken with  $V_m = -367$  mV and  $I_t = 0.54$  nA. (c) A schematic diagram of the zigzag configuration of the nanotubule in which the large circles represent the atoms observed in the STM image. (d) A  $150 \times 150$  nm overview on another sample surface. The bias is  $V_m = -476$  mV and the tunnelling current of  $I_t = 0.23$  nA. (e) An atomic scale image of  $42 \times 42$  Å on one tubule in (d). The image was taken with  $V_m = -228$  mV and  $I_t = 0.60$  nA. (f) A schematic diagram of the armchair configuration of the nanotubule in which the large circles are also representative of the surface atoms observed in the STM image.

graphite, and an upper part with an extended row feature. One direction of the atom rows is determined to be identical to that of the tubule axis, at  $\sim 15^\circ$  from the horizontal of the picture, and the row spacing is  $\sim 2.1$  Å, similar to that in the STM image of graphite. These results indicate that the imaged nanotubule is in the armchair configuration, where one C–C bond in hexagons of the nanotubes is perpendicular to the tubule axis. In Fig. 3(f) a schematic diagram of the armchair configuration of the nanotubule is also given. This identification of the armchair configuration, and that of the zigzag configuration given above, presents atomic resolution views and experimental evidence for the model of the tubule microstructures.

Around the middle of Fig. 3(e) it can be seen that the atom rows on the lower part appear to be nearly as

perfect as on graphite surface. But around the upper part, elongated image spots are observed, which seemingly extend from those rows in the lower part. These elongated spots can be considered as resulting from variations of the local electronic states on the nanotubule surface, that can be induced by lattice mismatches between the surface and the layer beneath. Between the lower and upper atom rows there exists a transition region with a width of about one C–C bond length. This transition suggests a sharp bending of the graphitic layers along the boundary line, which can be formed by folding graphite sheets to create the tubular shape of the nanotubes. Due to the bending, the lengths and angles of C–C bonds in the hexagons can be varied around the boundary line. This can considerably affect the local distribution of electronic

states there and lead to variations of the STM images of nanotubes from that of graphite. These structural variations will be investigated in a further study.

#### 4. Summary

We have performed spectroscopy studies on morphologies and structures of carbon nanotubes and onions using SEM, HRTEM and STM. The SEM observations show where the nanotubes and onions are produced in the carbon deposit of arc discharge and that their general morphology is similar to that of some carbon fibrous whiskers grown from pyrolytic graphite. The high resolution TEM results provide support for the growth mechanism. In addition, the HRTEM observation shows that the graphitic sheets can be bent in a curved shape to cap the nanotubes or form the onions. In the apex of the enclosure cap, elastic strains induced by layer mismatches and dislocations are involved which produce particular features in the HRTEM images. The bundle-like morphology of the carbon nanotubes has been observed by STM where the tubules appear to align in the same direction. By atomic resolution images two main atomic orientations, i.e., the zigzag and arm-chair configurations, are observed and variations of the image features from that of graphite, due to the

layer mismatch in the nanotubes, are shown. The results also show structural distortions which may be produced by folding the graphite sheets to create the nanotubes and may be responsible for the lattice mismatch.

#### References

1. S. IIJIMA, *Nature* **354** (1991) 56.
2. S. IIJIMA, T. ICHIHASHI and Y. ANDO, *ibid.* **356** (1992) 776.
3. S. IIJIMA, P. M. AJAYAN and T. ICHIHASHI, *Phys. Rev. Lett.* **69** (1992) 3100.
4. P. M. AJAYAN and S. IIJIMA, *Nature* **358** (1992) 23.
5. T. LENOSKY, X. GONZE, M. TETER and V. ELSER, *ibid.* **355** (1992) 333.
6. N. HAMADA, SHIN-ICHI SAWADA and A. OSHIYAMA, *Phys. Rev. Lett.* **68** (1992) 1579.
7. R. SAITO, M. FUJITA, G. DRESSELHAUS and M. S. DRESSELHAUS, *Appl. Phys. Lett.* **60** (1992) 2204.
8. T. W. EBBESEN and P. M. AJAYAN, *Nature* **358** (1992) 220.
9. NAN LI, SHENGFA QIAN, CHUNSHENG FU, GANG WANG and SISHEN XIE, *Appl. Phys. Lett.*, in press.
10. V. P. DRAVID, X. LIN, Y. WANG, A. YEE, J. B. KETTERSON and R. P. H. CHANG, *Science* **259** (1993) 1601.

*Received 8 April  
and accepted 4 October 1994*